Introduction to colloidal systems

Daan Frenkel

FOM Institute for Atomic and Molecular Physics, The Netherlands

1 Introduction

Karl Marx has said that, in history, things always happen twice: the first time as a tragedy, the second time as a farce. This comment of Marx applied to Napoleon I and III. However, if we strip the subjective interpretation (tragedy or farce) from this sentence, it could apply to many phenomena in physics. In physics, there often appears to be a similarity between phenomena on very different length and time-scales but, on closer inspection, there are important, even qualitative differences. Examples abound: in some respects, light waves resemble ripples on a pond but, in most respects, they are totally different. The Bohr model of the atom resembled a planetary system but, of course, the differences are so important that, in the end, they led to the demise of the Bohr model. These two examples illustrate an important point: in physics, analogies are very useful in formulating an approximate description of a phenomenon—but even more interesting than the analogy itself, is its breakdown.

In many ways, colloids behave like giant atoms, and quite a bit of the colloid physics can be understood in this way. However, much of the interesting behaviour of colloids is related to the fact that they are, in many respects, *not* like atoms. In these lectures, I shall start from the picture of colloids as oversized atoms or molecules, and then I shall selectively discuss some features of colloids that are different. My presentation of the subject might seem a bit strange, because I am a computer simulator, rather than a colloid scientist. Colloids are the computer simulator's dream, because many of them can be represented quite well by models—such as the hard-sphere and Yukawa models—that are far too simple to represent molecular systems. On the other hand, colloids are also the simulator's nightmare, or at least challenge, because if we look more closely, simple models do not work: this is sometimes true for the static properties of colloids (*e.g.* in the case of charged colloids) and even more often, in the case of colloid dynamics.

What are colloids? Usually, we refer to a substance as a colloidal suspension if it is a dispersion of more-or-less compact particles with sizes within a certain range (typically, 1nm–1μm). However, it would be more logical to classify colloids according to some phys-

ical criterion. To this end, we should compare colloidal particles with their 'neighbours': small molecules on one end of the scale, and bricks on the other. What distinguishes colloids from small molecules? I would propose that the important difference is that for the description of colloids, a detailed knowledge of the 'internal' degrees of freedom is not needed—in particular, the discrete, atomic nature of matter should be irrelevant. That is *not* to say that the chemical nature of the constituent atoms or molecules is irrelevant—simply that, in order to describe a colloid, we do not need to know the detailed microscopic arrangement of these constituents. This definition has the advantage that it allows for the fact that particles may behave like colloids in some respects, and like 'molecules' in others. For instance, we cannot hope to understand the biological function of proteins if we do not know their atomic structure. However, we can understand a lot about the phase behaviour of proteins without such knowledge. This ambiguous nature of macromolecules may persist even at length scales that are usually considered colloidal. For instance, for the biological function of the Tobacco Mosaic Virus, the precise sequence of its genetic material is important. But its tendency to form colloidal liquid crystals depends only on coarse-grained properties, such as shape, flexibility and charge.

Let us next consider the other side of the scale. What is the difference between a colloidal particle and a brick? The behaviour of colloids is governed by the laws of statistical mechanics. In equilibrium, colloidal suspensions occur in the phase with the lowest free energy, and the dynamics of colloids in equilibrium is due to thermal (Brownian) motion. In principle, this should also be true for bricks. But in practice, it is not. In order for bricks to behave like colloids, they should be able to evolve due to Brownian motion. There are two reasons why bricks do not. First of all, on earth, all particles are subject to gravity. The probability of finding a particle of mass m at a height h above the surface of the earth is given by the barometric height distribution:

$$P(h) = \exp(-mgh/k_BT) \ , \tag{1}$$

where m is the effective mass of the colloidal particle (*i.e.* the mass, minus the mass of the displaced solvent), T is the temperature and k_B is Boltzmann's constant. The average height of the colloid above the surface is equal to $\langle h \rangle = k_BT/(mg)$. For a 1kg brick at room temperature, $\langle h \rangle = O(10^{-20})$ cm. This tells us something that we all know: bricks don't float around due to thermal motion. One way to delimit the colloidal regime is to require that $\langle h \rangle$ is larger than the particle diameter. Suppose we have a spherical particle with diameter σ and (excess) mass density ρ, then our criterion implies

$$\frac{\pi g \rho \sigma^4}{6} = k_BT \ . \tag{2}$$

For a particle with an excess density of $1\mathrm{g/cm}^3$, the above equality is satisfied for a value of $\sigma \approx 1\mu$m, *i.e.* on earth. In the microgravity environment that prevails in space, much larger particles would behave like colloids (not bricks though, because it is virtually impossible to reduce all accelerations to less than $10^{-20}g$). Another way to make large particles behave like colloids on earth, is to match the density of the solvent to that of the particle. Yet, even if we could succeed in doing all this for a brick, it would still not behave like a colloid. Colloidal particles should be able to move due to diffusion (*i.e.* thermal motion). How long does it take for a particle to move a distance equal to its own diameter? In a time t, a particle typically diffuses a distance $\sqrt{2Dt}$. For a spherical

particle, the diffusion constant is given by the Stokes-Einstein relation $D = k_B T/(3\pi\eta\sigma)$, where η is the viscosity of the solution. Hence, a particle diffuses a distance comparable to its own diameter in a time

$$\tau = O(\eta\sigma^3/k_B T) \; . \tag{3}$$

For a $1\mu m$-colloid in water, this time is of the order of one second. For a brick, it is of the order of ten million years. Hence, even though bricks in zero-gravity may behave like colloids, they will not do so on a human time-scale. Clearly, what we define as a colloid, also depends on the observation time. Again, 1 micron comes out as a natural upper limit to the colloidal domain.

In summary, a colloid is defined by its behaviour. For practical purposes, the colloidal regime is between 1 nanometre and 1 micrometre. But these boundaries are not sharp. And the lower boundary is ambiguous: a particle may behave like a colloid in some respects, but not in others.

2 Forces between colloids

Most colloidal suspensions are solutions of relatively large particles in a simple molecular solvent. Yet, the description of the static properties of such a solution resembles that of a system of atoms in vacuum—somehow, the solvent does not appear explicitly. At first sight, this seems like a gross omission. However, as pointed out by Onsager [1], we can eliminate the degrees of freedom of the solvent in a colloidal dispersion. What results is the description that only involves the colloidal particles, interacting through some *effective* potential (the 'potential of mean force') that accounts for all solvent effects. Below, I briefly sketch how this works. Consider a system of N_c colloids in a volume V at temperature T. The solvent is held at constant chemical potential μ_s, but the number of solvent molecules N_s is fluctuating. The 'semi-grand' partition function of such a system is (with $\beta = 1/k_B T$)

$$\Xi(N_c, \mu_s, V, T) \equiv \sum_{N_s=0}^{\infty} \exp(\beta\mu_s N_s) Q(N_c, N_s, V, T) \; . \tag{4}$$

The canonical partition function $Q(N_c, N_s, V, T)$ is given by the classical expression for a mixture

$$Q(N_c, N_s, V, T) = \frac{q_{\mathrm{id},c}(T)^{N_c} q_{\mathrm{id},s}(T)^{N_s}}{N_c! N_s!} \int dr^{N_c} dr^{N_s} \exp[-\beta U(r^{N_c}, r^{N_s})] \; . \tag{5}$$

where $q_{\mathrm{id},\alpha}$ is the kinetic and intra-molecular part of the partition function of a particle of species α, and r^{N_c} (r^{N_s}) denotes a $3N_c$ ($3N_s$) dimensional vector specifying a complete set of colloid (solvent) coordinates. The $q_{\mathrm{id},\alpha}$ terms are assumed to depend only on temperature, and not on the inter-molecular interactions (sometimes this is not true, *e.g.* in the case of polymers—I shall come back to that point later). In what follows, I shall usually drop the factors $q_{\mathrm{id},\alpha}$ (more precisely, I shall account for them in the definition of the chemical potential: *i.e.* $\mu_\alpha \to \mu_\alpha + k_B T \ln q_{\mathrm{id},\alpha}$). The interaction potential $U(r^{N_c}, r^{N_s})$ can always be written as $U_{cc} + U_{ss} + U_{sc}$, where U_{cc} is the direct colloid-colloid interaction

(*i.e.* $U(r^{N_c}, r^{N_s})$ for $N_s = 0$), U_{ss} is the solvent-solvent interaction (*i.e.* $U(r^{N_c}, r^{N_s})$ for $N_c = 0$), and U_{sc} is the solvent-colloid interaction $U(r^{N_c}, r^{N_s}) - U_{cc}(r^{N_c}) - U_{ss}(r^{N_s})$. With these definitions, we can write

$$Q(N_c, N_s, V, T) = \frac{1}{N_c!} \int dr^{N_c} \exp[-\beta U_{cc}] \left\{ \frac{1}{N_s!} \int dr^{N_s} \exp[-\beta(U_{ss} + U_{sc})] \right\} \quad (6)$$

and hence

$$\Xi(N_c, \mu_s, V, T) = \frac{1}{N_c!} \int dr^{N_c} \exp[-\beta U_{cc}] \times \left\{ \sum_{N_s=0}^{\infty} \frac{\exp(\beta \mu_s N_s)}{N_s!} \int dr^{N_s} \exp[-\beta(U_{ss} + U_{sc})] \right\} . \quad (7)$$

We can rewrite this in a slightly more suggestive form. If we define the usual canonical and grand-canonical partition functions for solvent alone as

$$Q_s(N_s, V, T) \equiv \frac{1}{N_s!} \int dr^{N_s} \exp[-\beta U_{ss}] , \quad (8)$$

$$\Xi(\mu_s, V, T) \equiv \sum_{N_s=0}^{\infty} \exp(\beta \mu_s N_s) Q_s(N_s, V, T) , \quad (9)$$

then

$$\begin{aligned} \Xi(N_c, \mu_s, V, T) &= \frac{1}{N_c!} \int dr^{N_c} \exp[-\beta U_{cc}] \\ &\quad \times \left\{ \sum_{N_s=0}^{\infty} \exp(\beta \mu_s N_s) Q_s(N_s, V, T) \left\langle \exp[-\beta U_{sc}] \right\rangle_{N_c, N_s, V, T} \right\} \\ &= \frac{\Xi(\mu_s, V, T)}{N_c!} \int dr^{N_c} \exp[-\beta U_{cc}] \left\langle \exp[-\beta U_{sc}] \right\rangle_{\mu_s, T} , \end{aligned} \quad (10)$$

where

$$\left\langle \exp[-\beta U_{sc}] \right\rangle_{\mu_s, V, T} \equiv \frac{\sum_{N_s=0}^{\infty} \exp(\beta \mu_s N_s) Q_s(N_s, V, T) \left\langle \exp[-\beta U_{sc}] \right\rangle_{N_c, N_s, V, T}}{\Xi(\mu_s, V, T)} . \quad (11)$$

Note that this quantity still depends on all the colloid coordinates, r^{N_c}: it is the average over solvent coordinates of the Boltzmann factor for the solvent-colloid interaction. We now define the *effective* colloid-colloid interaction as

$$U_{cc}^{\text{eff}}(r^{N_c}) \equiv U_{cc}(r^{N_c}) - k_B T \ln \left\langle \exp[-\beta U_{sc}(r^{N_c})] \right\rangle_{\mu_s, V, T} . \quad (12)$$

We refer to $U_{cc}^{\text{eff}}(r^{N_c})$ as the *potential of mean force*. Note that the potential of mean force depends explicitly on the temperature and on the chemical potential of the solvent. In the case where we study colloidal suspensions in *mixed* solvents, the potential of mean force depends on the chemical potential of all components in the solvent (an important example is a colloidal dispersed in a polymer solution).

At first sight, it looks as if the potential of mean force is a totally intractable object. For instance, even when the colloid-solvent and solvent-solvent interactions are pairwise

additive, the potential of mean force is not. (Note that we have, thus far, not even assumed pairwise additivity). However, we should bear in mind that even the 'normal' potential energy function that we all think we know and love, is also not pairwise additive—that is why we can hardly ever use the pair potentials that describe the intermolecular interactions in the gas phase to model simple liquids. In fact, in many cases, we can make very reasonable estimates of the potential of mean force. It also turns out that the dependence of the potential of mean force on the chemical potential of the solvent molecules is a great advantage: it will allow us to *tune* the effective forces between colloids *simply by changing the composition of the solvent.* (You all know this: simply add some vinegar to milk, and the colloidal fat globules in the milk start to aggregate.) In contrast, in order to change the forces between atoms in the gas phase, we would have to change Planck's constant or the mass or charge of an electron. Hence, colloids are not simply giant atoms, they are *tunable* giant atoms.

We shall now briefly review the nature of inter-colloidal interactions. It will turn out that, almost all colloid-colloid interactions depend on the nature of the solvent and are, therefore, potentials of mean force.

2.1 Hard-core repulsion

Colloidal particles tend to have a well-defined size and shape. They behave like solid bodies—in fact, many colloidal particles *are* fairly solid (*e.g.* the colloids that Perrin used to determine Avogadro's number were small rubber balls, silica colloids are small glass spheres and PMMA colloids are made out of plastic). Solid bodies cannot interpenetrate. This property can be related to the fact that, at short range, the interaction between (non-reactive) atoms is harshly repulsive. This is due to the Pauli exclusion principle. This hard-core repulsion is about the only colloid-colloid interaction that is essentially independent of the solvent. In fact, colloidal crystals can be dried and studied in the electron microscope because the Pauli exclusion principle works just as well in vacuum as in solution. However, there are also other mechanisms that lead to 'hard-core' repulsion in colloids: for instance, short-ranged Coulomb-repulsion between like-charged colloids, or entropic repulsion between colloids that have a polymer 'fur', or even solvent-induced repulsion effects. All these repulsion mechanisms are sensitive to the nature of the solvent. We shall come back to them later.

2.2 Coulomb interaction

The Coulomb interaction would seem to be the prototype of a simple, pairwise additive interaction. In fact, it is. However, for every charge carried by the colloidal particles, there is a compensating charge in the solvent. These counter charges 'screen' the direct Coulomb repulsion between the colloids. I put the word 'screen' in quotes because it is too passive a word to describe what the counterions do: even in the presence of counterions and added salt ions the direct, long-ranged Coulomb repulsion between the colloids exists—but it is almost completely compensated by a net attractive interaction due to the counterions. The net result is an *effective* interaction between the colloids that is short-ranged *i.e.* it decays asymptotically as $\exp(-\kappa r)/r$, with κ the inverse screening length ($\kappa = 1/r_D$) that

appears in the Debye-Hückel theory of electrolytes:

$$\kappa = \sqrt{\frac{4\pi}{\epsilon k_B T} \sum_i \rho_i q_i^2} \ ,$$

where ϵ is the dielectric constant of the solvent and ρ_i is the number density of ionic species i with charge q_i. (Here, and below, we used rationalised units for electrostatics, rather than SI units).

The first expression for the effective electrostatic interaction between two charged colloids was proposed Derjaguin, Landau, Verweij and Overbeek (DLVO) [2]:

$$V_{\text{Coulomb}} = \left(\frac{Q \exp(\kappa R)}{1+\kappa R}\right)^2 \frac{\exp(-\kappa r)}{\epsilon r} \ , \tag{13}$$

where r is the distance between the two charged colloids, Q is the (bare) charge of the colloid and R is its 'hard-core' radius. Ever since, there have been attempts to improve on the DLVO theory. However, the theory of the effective electrostatic interaction between colloids is subtle and full of pitfalls. Usually, the electrostatic interaction between like-charged colloids is repulsive. However, under certain conditions it can be attractive. Sogami and Ise [3] have reported many experiments that provide evidence for such attraction. These authors suggested that this attraction should even be present at the level of the effective pair interaction. Recently, however, detailed experimental information has become available [4] that suggests that the Coulomb attraction between like-charged colloids is *not* present in the interaction between an isolated pair of colloids in the bulk solvent. At present, experiment and theory both suggest that all attractive interactions are either mediated by the presence of confining walls [5–7], (but see, however, [8]) or, in the bulk, they are due to many-body effects [9]. In addition, fluctuations in the charge distribution on the colloids may lead to dispersion-like attractive interactions (see *e.g.* [10]) that are also non-pairwise additive. Having said all this, the old DLVO theory usually yields an excellent first approximation for the electrostatic interaction between charged colloids.

2.3 Dispersion forces

Dispersion forces are due to the correlated zero-point fluctuations of the dipole moments on atoms or molecules. As colloids consist of many atoms, dispersion forces act between colloids. However, it would wrong to conclude that the solvent has no effect on the dispersion forces acting between colloids. After all, there are also dispersion forces acting between the colloids and the solvent, and between the solvent molecules themselves. In fact, for a pair of polarisable molecules, the dispersion interaction depends on the polarisabilities (α_1 and α_2) of the individual particles

$$u_{\text{disp}}(r) \sim -\frac{3\alpha_1\alpha_2 h\sqrt{\nu_1\nu_2}}{4\pi r^6} \equiv -\frac{C_{\text{disp}}(12)}{r^6} \ , \tag{14}$$

where $h\nu_i$ is a characteristic energy associated with the optical transition responsible for the dipole fluctuations in molecule i (in what follows, we shall assume the frequency ν_i to be the same for all molecules). The net dispersion force between colloidal particles

in suspension depends on the difference in polarisability per unit volume of the solvent and the colloid. The reason is easy to understand: if we insert two colloidal particles in a polarisable solvent, we replace solvent with polarisability density $\rho_s\alpha_s$ by colloid with polarisability density $\rho_c\alpha_c$. If the two colloidal particles are far apart, each colloid contributes a constant amount proportional to $-\rho_s\alpha_s(\rho_c\alpha_c-\rho_s\alpha_s)$ to the dispersion energy. However, if at short inter-colloidal distances there is an additional *effective* colloid-colloid interaction that is proportional to $-(\rho_c\alpha_c-\rho_s\alpha_s)^2/r_{cc}^6$, then this leads to an *attractive interaction* irrespective of whether the polarisability density of the colloids is higher or lower than that of the solvent. On the other hand, in a colloid mixture, the dispersion force need not be attractive: if the polarisability density of one colloid (denoted by $c1$) is *higher* than that of the solvent, and the polarisability density of the other (denoted by $c2$) is *lower*, then the positive-definite square $(\rho_c\alpha_c-\rho_s\alpha_s)^2$ is replaced by the negative product $(\rho_{c1}\alpha_{c1}-\rho_s\alpha_s)(\rho_{c2}\alpha_{c2}-\rho_s\alpha_s)$ and hence the effective dispersion forces between these two colloids are *repulsive*.

The polarisability density of bulk phases is directly related to the refractive index. For instance, the Clausius-Mosotti expression for the refractive index is

$$\frac{n^2-1}{n^2+2}=\frac{4\pi\rho\alpha}{3}. \tag{15}$$

Hence, if the refractive index of the solvent is equal to that of the colloidal particles, then the effective dispersion forces vanish! This procedure to switch off the effective dispersion forces is called *refractive index matching*. In light-scattering experiments on dense colloidal suspensions, it is common to match the refractive indices of solvent and colloid in order to reduce multiple scattering. Thus, precisely the conditions that minimise the dispersion forces are optimal for light-scattering experiments.

Colloids are not point particles, therefore Equation 14 has to be integrated over the volumes of the interacting colloids, to yield the total dispersion interaction

$$V_{\text{disp}}(r)=-\frac{A}{6}\left\{\frac{2R^2}{r^2-4R^2}+\frac{2R^2}{r^2}+\ln\frac{r^2-4R^2}{r^2}\right\}, \tag{16}$$

where A is the so-called *Hamaker constant*. In the simple picture sketched above, A would be proportional to $(\rho_c\alpha_c-\rho_s\alpha_s)^2$. However, in a more sophisticated theoretical description of the dispersion forces between macroscopic bodies (see *e.g.* the book by Israelachvili [11]), the Hamaker constant can be related explicitly to the (frequency-dependent) dielectric constants of the colloidal particles and the solvent. This analysis affects the value of the constant A but, to a first approximation, not the functional form of Equation 16.

2.4 DLVO potential

Combining Equations 13 and 16, we obtain the DLVO potential that describes the interaction between charged colloids

$$V_{DLVO}(r)=\left(\frac{Q\exp(\kappa R)}{1+\kappa R}\right)^2\frac{\exp(-\kappa r)}{\epsilon r}-\frac{A}{6}\left\{\frac{2R^2}{r^2-4R^2}+\frac{2R^2}{r^2}+\ln\frac{r^2-4R^2}{r^2}\right\}. \tag{17}$$

This potential is shown in Figure 1. Note that, at short distances, the dispersion forces always win. This suggests that the dispersion interaction will always lead to colloidal

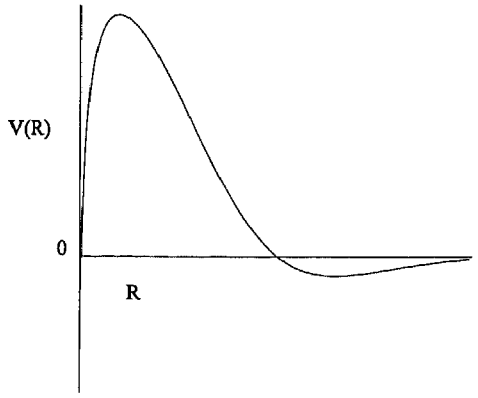

Figure 1. *The DLVO potential has a deep minimum at short distances. At larger distances, the Coulomb repulsion dominates. This leads to the local maximum in the curve. At still larger distances, the dispersion interaction may lead to a secondary minimum.*

aggregation. However, the electrostatic repulsion usually prevents colloids from getting close enough to fall into the primary minimum of the DLVO potential. The height of this stabilising barrier depends (through κ) on the salt concentration. Adding more salt will lower the barrier and, eventually, the colloids will be able to cross the barrier and aggregate.

Density matching—an intermezzo

In addition to refractive index matching, it is useful to try to match the density of the solvent to that of the colloid. This has an utterly negligible effect on the interaction between colloids. But, as far as gravity is concerned, density-matched colloidal particles are neutrally buoyant—that is they behave as if they have a very small (ideally zero) positive or negative excess mass. This is the mass that enters into the barometric height distribution (Equation 1). Hence, by density-matching, we can study bulk suspensions of colloids that would otherwise quickly settle on the bottom of the container.

2.5 Depletion interaction

One of the most surprising effects of the solvent on the interaction between colloids, is the so-called depletion interaction. Unlike the forces that we have discussed up to this point, the depletion force is not a solvent-induced modification of some pre-existing force between the colloids. It is a pure solvent effect. It is a consequence of the fact that the colloidal particles exclude space from the solvent molecules. To understand it, return to Equation 12:

$$U_{cc}^{\text{eff}}(r^{N_c}) \equiv U_{cc}(r^{N_c}) - k_B T \ln \left\langle \exp[-\beta U_{sc}(r^{N_c})] \right\rangle_{\mu_s,V,T} \quad .$$

Let us consider a system of hard particles with no additional attractive or repulsive interaction. In that case, all the contributions to the second term of the *effective* potential

in Equation 12 are depletion interactions. These interactions can be attractive, even though all direct interactions in the system are repulsive.

To illustrate this, consider a trivial model system, namely a 2-dimensional square lattice with at most one particle allowed per square [12].

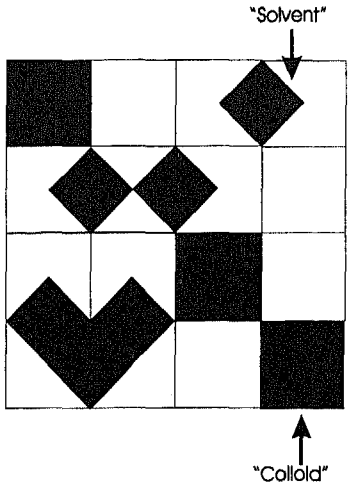

Figure 2. *Two-dimensional lattice model of a hard-core mixture of large colloidal particles (grey squares) and small solvent particles (black squares). Averaging over the solvent degrees of freedom results in a net attractive interaction (depletion interaction) between the 'colloids'.*

Apart from the fact that no two particles can occupy the same square cell, there is no interaction between the particles. For a lattice of N sites, the grand-canonical partition function is:

$$\Xi = \sum_{\{n_i\}} \exp[\beta\mu_c \sum_i n_i] \,. \tag{18}$$

The sum is over all allowed sets of occupation numbers $\{n_i\}$ and μ_c is the chemical potential of the 'colloidal' particles. Next, we include small 'solvent' particles that are allowed to sit on the links of the lattice (see Figure 2). These small particles are excluded from the edges of a cell that is occupied by a large particle. For a given configuration $\{n_i\}$ of the large particles, one can then calculate exactly the grand canonical partition function of the small particles. Let $M = M(\{n_i\})$ be the number of free spaces accessible to the small particles. Then clearly:

$$\Xi_{\text{small}}(\{n_i\}) = \sum_{l=0}^{M} \frac{M! z_s^l}{l!(M-l)!} = (1+z_s)^{M(\{n_i\})}, \tag{19}$$

where $z_s \equiv \exp(\beta\mu_s)$ is the fugacity of the small particles. M can be written as

$$M(\{n_i\}) = Nd - 2d\sum_i n_i + \sum_{\langle ij \rangle} n_i n_j \,, \tag{20}$$

where we have given the result for general space dimension d; Nd is the number of links on the lattice and the second sum is over nearest-neighbour pairs and comes from the fact that when two large particles touch, the number of sites excluded for the small particles is $4d-1$, not $4d$. Whenever two large particles touch, we have to correct for this overcounting of excluded sites. The total grand-partition function for the mixture is:

$$\Xi_{\text{mixture}} = \sum_{\{n_i\}} \exp\left[(\beta\mu_c - 2d\log(1+z_s))\sum_i n_i + [\log(1+z_s)]\sum_{\langle ij\rangle} n_i n_j\right], \qquad (21)$$

where we have omitted a constant factor $(1+z_s)^{Nd}$. Now we can bring this equation into a more familiar form by using a standard procedure to translate a lattice-gas model into a spin model. We define spins s_i such that $2n_i - 1 = s_i$ or $n_i = (s_i+1)/2$. Then we can write Equation 21 as

$$\Xi_{\text{mixture}} = \sum_{\{n_i\}} \exp\left[\frac{\beta\mu_c - d\log(1+z_s)}{2}\sum_i s_i + \frac{\log(1+z_s)}{4}\sum_{\langle ij\rangle} s_i s_j + \text{const.}\right]. \qquad (22)$$

This is simply the expression for the partition function of an Ising model in a magnetic field with strength $H = (\mu_c - d\log(1+z_s)/\beta)$ and an effective nearest neighbour *attraction* with an interaction strength $J = \log(1+z_s)/(4\beta)$.

There is hardly a model in physics that has been studied more than the Ising model. In two dimensions, the partition function can be computed analytically in the zero field case [13]. In the language of our mixture model, no external magnetic field means:

$$(1+z_s)^d = z_c, \qquad (23)$$

where $z_c = \exp\beta\mu_c$, the large particle fugacity.

Several points should be noted. First of all, in this simple lattice model, summing over all solvent degrees of freedom resulted in effective *attractive* nearest neighbour interaction between the hard-core colloids. Secondly, below its critical temperature, the Ising model (for $d > 1$) exhibits spontaneous magnetisation. In the mixture model, this means that, above a critical value of the fugacity of the solvent, there will be phase transition in which a phase with low $\langle n_c\rangle$ (a dilute colloidal suspension) coexists with a phase with high $\langle n_c\rangle$ (concentrated suspension). Hence, this model system with purely repulsive hard-core interaction can undergo a demixing transition. This demixing is purely entropic.

2.6 Depletion flocculation

Let us next consider a slightly more realistic example of an entropy-driven phase separation in a binary mixture, namely polymer-induced flocculation of colloids. Experimentally, it is well known that the addition of a small amount of free, non-adsorbing polymer to a colloidal suspension induces an effective attraction between the colloidal particles and may even lead to coagulation. This effect has been studied extensively and is theoretically well understood [14–17]. As in the example discussed above, the polymer-induced attraction between colloids is an *entropic* effect: when the colloidal particles are close together, the total number of accessible polymer conformations is larger than when the colloidal particles are far apart.

To understand the depletion interaction due to polymers, let us again consider a system of hard-core colloids. To this system, we add a number of ideal polymers. Ideal, in this case means that, in the absence of the colloids, the polymers behave like an ideal gas. The configurational integral of a single polymer contains a translational part (V) and an intramolecular part, Z_{int}, which, for an ideal (non-interacting) polymer, is simply the sum over all distinct polymer configurations. In the presence of hard colloidal particles, only part of the volume of the system is accessible to the polymer. How much, depends on the conformational state of the polymer. This fact complicates the description of the polymer-colloid mixture, although numerically, the problem is tractable [18] .

To simplify matters, Asakura and Oosawa [14] introduced the assumption that, as far as the polymer-colloid interaction is concerned, the polymer behaves like a hard sphere with radius R_G. (Here R_G is the radius of gyration, which is comparable to other characteristic measures of polymer size, such as the RMS end-to-end distance; see Khokhlov, this volume.) What this means is that, as the polymer-colloid distance becomes less than R_G, most polymer conformations will result in an overlap with the colloid, but when the polymer-colloid distance is larger, most polymer conformations are permitted (this assumption has been tested numerically [18], and turns out to be quite good). As the polymers are assumed to be ideal, it is straightforward to write down the expression for the configurational integral of N_p polymers, in the presence of N_c colloids at fixed positions r^{N_c} :

$$\int dr^{N_p} \exp[-\beta(U_{ss} + U_{sc})] = \left\{ \int d\mathbf{r}_p \exp[-\beta U_{sc}(r^{N_c}; \mathbf{r}_p)] \right\}^{N_p} = V_{\text{eff}}^{N_p}(r^{N_c}) ,$$

where V_{eff} is the effective volume that is available to the polymers. Equation 10 then becomes

$$\begin{aligned} \Xi(N_c, \mu_s, V, T) &= \frac{1}{N_c!} \int dr^{N_c} \exp[-\beta U_{cc}(r^{N_c})] \sum_{N_p=0}^{\infty} \exp(\beta \mu_p N_p) \frac{V_{\text{eff}}^{N_p}(r^{N_c})}{N_p!} \\ &= \frac{1}{N_c!} \int dr^{N_c} \exp[-\beta U_{cc}(r^{N_c})] \exp(z_p V_{\text{eff}}(r^{N_c})) , \end{aligned} \tag{24}$$

where $z_p \equiv \exp(\beta \mu_p)$. Clearly, the effective colloid-colloid potential is now

$$U_{\text{eff}}(r^{N_c}) = U_{cc}(r^{N_c}) - \beta^{-1} z_p V_{\text{eff}}(r^{N_c}) . \tag{25}$$

This equation shows that the correction to the colloid-colloid interaction is due to the fact that the volume available to the polymers depends on the configuration of the colloids. The reason why this should be so is easy to understand. Consider two colloids of radius R at distance $r_1 \gg 2(R + R_G)$. In that case, every colloid excluded a spherical volume with radius $R + R_G$ to the polymers (see Figure 3).

Equation 25 shows that the depletion attraction increases with the polymer fugacity or, what amounts to the same thing, with the osmotic pressure of the polymers in solution. The more polymer we add to the suspension, the stronger the attraction. The range of the attraction depends on the size R_G of the polymers. The larger R_G, the longer the range of the attraction. If we model polymers as mutually interpenetrable spheres with radius R_G, then the explicit expression for the depletion interaction between a pair of

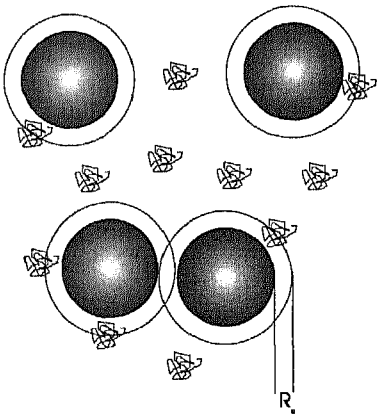

Figure 3. *Hard-core colloids exclude a shell with thickness R_G to the ideal polymers in the solution. When the colloids are far apart, the excluded volumes simply add up. At shorter distances, the excluded volumes overlap and the total volume available to the polymers increases.*

colloids is, for $2R < r < 2(R + R_G)$,

$$V_{\rm dep}(r) = -\frac{4\pi(R+R_G)^3 z_p k_B T}{3}\left\{1 - \frac{3r}{4(R+R_G)} + \frac{1}{16}\left(\frac{r}{R+R_G}\right)^3\right\}, \qquad (26)$$

where we have subtracted a constant term from the potential (namely the contribution of two colloids at a distance $r \gg 2(R + R_G)$). Equation 26 shows clearly that, by changing the size of the added polymers and their concentration, we can change both the range and the strength of the attractive interaction between the colloids. In Section 3, I shall discuss the effect of this tunable attraction on the phase behaviour of polymer-colloid mixtures.

One final comment is in place: the true depletion interaction is *not* pairwise additive. This is clear if we consider three colloidal spheres: if the three exclusion zones overlap, the total excluded volume is larger than would be estimated on basis of the pair-terms alone. Hence, three-body forces yield a *repulsive* correction to the depletion interaction. Note that three-body forces are only important if R_G/R is large enough to get the three exclusion zones to overlap. This holds *a fortiori* for the 4-body forces (that are, again, attractive), *etc.* This feature of the depletion interaction does not depend on the details of the Asakura-Oosawa model. In fact, direct simulations of hard colloids and (lattice) polymers [18] show exactly the same effect.

2.7 Why colloidal materials are soft

Let me return to the picture of colloids as giant atoms. We now know that this is an oversimplification—the origins of the effective interaction between colloids often have no counterpart in atomic physics. Yet, if we ignore all these subtleties, there are similarities. Both atoms and colloids have an effective hard-core diameter: σ_a for atoms, σ_c for colloids. Typically, $\sigma_c/\sigma_a = \mathcal{O}(10^3)$. The characteristic interaction energies between

colloids ε_c are of the order of the thermal energy k_BT. For atomic solids, the interaction energy ε_a depends on the nature of the interatomic interaction: it may vary from a value comparable to k_BT for van der Waals crystals, to a value of the order of electron-volts for covalently bonded materials (*e.g.* diamond). Knowing the characteristic sizes and the characteristic interaction energies of the particles, is enough to give an order-of-magnitude estimate of various physical properties (basically, this is simply an over-extension of van der Waals' Law of Corresponding States). For instance, the elastic constants of a solid have the dimensions [energy/volume]. That means that the elastic constants of a dense colloidal suspension are of the order k_BT/σ_c^3. For an atomic van der Waals solid, the elastic constants are of the order k_BT/σ_a^3. In other words: the force needed to deform a colloidal crystal is a factor $\sigma_c^3/\sigma_a^3 \approx 10^9$ smaller than for an atomic crystal held together by dispersion forces (and these are the softest atomic crystals). Clearly, colloidal matter is very easily deformable; it is indeed 'soft matter'.

2.8 Polydispersity

All atoms of a given type are identical. They have the same size, weight and interaction strength. This is usually not true for colloids. In fact, all synthetic colloids are to some degree polydisperse, *i.e.* they do not all have the same size (or mass, or shape, or refractive index). This polydispersity is usually a complicating factor: it makes it more difficult to interpret experimental data (*e.g.* X-ray or neutron scattering, or dynamic light-scattering). In addition, it may broaden phase coexistence regions and, in some cases even completely wipe out certain phases. However, polydispersity is not all bad: it also leads to interesting new physics. For instance, sometimes polydispersity may induce a new phase that is not stable in the monodisperse limit [19]. In general, the effect of polydispersity on the stability of phases is most pronounced in the high-density limit. In that limit, polydispersity may lead to a frustration of the local packing.

3 Colloidal phase behaviour

In Section 2, I explained that the interactions between colloids can often be *tuned*. It is possible to make (uncharged, refractive-index matched, sterically stabilised) colloids that have a steep repulsive interaction and no attraction. These colloids behave like the hard-core models that have been studied extensively in computer simulation of simple fluids. But it is also possible to make (charged) colloids with smooth, long-ranged repulsion. And, using for instance, added polymer to induce a depletion interaction, colloids can be made with variable ranged attractions. Finally, colloids need not be spherical. It is possible to make colloidal rods and disks. Below, I briefly discuss some of the interesting consequences that this freedom to design the colloid-colloid interaction has for the phase behaviour.

3.1 Entropic phase transitions

The second law of thermodynamics tells us that any spontaneous change in a closed system results in an increase of the entropy, S. In this sense, all spontaneous transformations of

one phase into another are entropy driven. However, this is not what the term 'entropic phase transitions' is meant to describe. It is more common to consider the behaviour of a system that is not isolated, but can exchange energy with its surroundings. In that case, the second law of thermodynamics implies that the system will tend to minimise its Helmholtz free energy $F = E - TS$, where E is the internal energy of the system and T the temperature. Clearly, a system at constant temperature can lower its free energy in two ways: either by *increasing* the entropy S, or by *decreasing* the internal energy E.

In order to gain a better understanding of the factors that influence phase transitions, we must look at the statistical mechanical expressions for entropy. The simplest starting point is to use Boltzmann's expression for the entropy of an isolated system of N particles in volume V at an energy E,

$$S = k_B \ln \Omega \,, \tag{27}$$

where k_B, the Boltzmann constant, is simply a constant of proportionality. Ω is the total number of (quantum) states that is accessible to the system. In the remainder of these lecture notes, I shall often choose my units such that k_B=1. The usual interpretation of Equation 27 is that Ω, the number of accessible states of a system, is a measure for the disorder in that system. The larger the disorder, the larger the entropy. This interpretation of entropy suggests that a phase transition from a disordered to a more ordered phase can only take place if the loss in entropy is compensated by the decrease in internal energy. This statement is completely correct, provided that we use Equation 27 to *define* the amount of disorder in a system. However, we also have an *intuitive* idea of order and disorder: we consider crystalline solids ordered, and isotropic liquids disordered. This intuitive picture suggests that a spontaneous phase transition from the fluid to the crystalline state can only take place if the freezing lowers the internal energy of the system sufficiently to outweigh the loss in entropy: *i.e.* the ordering transition is 'energy driven'. In many cases, this is precisely what happens. It would, however, be a mistake to assume that our intuitive definition of order always coincides with the one based on Equation 27. In fact, the aim of this section is to show that many 'ordering' transitions that are usually considered to be energy-driven may, in fact, be entropy driven. I stress that the idea of entropy-driven phase transitions is an old one. However, it has only become clear during the past few years that such phase transformations may not be interesting exceptions, but the rule!

In order to observe 'pure' entropic phase transitions, we should consider systems for which the internal energy is a function of the temperature, but not of the density. Using elementary statistical mechanics, it is easy to show that this condition is satisfied for classical hard-core systems. Whenever these systems order at a fixed density and temperature, they can only do so by increasing their entropy (because, at constant temperature, their internal energy is fixed). Such systems are conveniently studied in computer simulations. But, increasingly, experimentalists—in particular, colloid scientists, have succeeded in making real systems that behave very nearly as ideal hard-core systems [24]. Hence, the phase transitions discussed below can, and in many cases, do occur in nature. Below I list examples of entropic ordering in hard-core systems. But I stress that the list is far from complete.

3.2 Computer simulation of (liquid) crystals

The earliest example of an entropy-driven ordering transition is described in a classic paper of Onsager [1], on the isotropic-nematic transition in a (three-dimensional) system of thin hard rods. Onsager showed that, on compression, a fluid of thin hard rods of length L and diameter D *must* undergo a transition from the isotropic fluid phase, where the molecules are translationally and orientationally disordered, to the nematic phase. In the latter phase, the molecules are translationally disordered, but their orientations are, on average, aligned. This transitions takes place at a density such that $(N/V)L^2D$ is of order unity. Onsager considered the limit $L/D \to \infty$. In this case, the phase transition of the hard-rod model can be found exactly [33]. At first sight it may seem strange that the hard rod system can *increase* its entropy by going from a disordered fluid phase to an orientationally ordered phase. Indeed, due to the orientational ordering of the system, the orientational entropy of the system decreases. However, this loss in entropy is more than offset by the increase in translational entropy of the system: the available space for the centre of any one rod increases as the rods become more aligned. In fact, we shall see this mechanism returning time and again in ordering transitions of hard-core systems: the entropy *decreases* because the density is no longer uniform in orientation or position, but the entropy *increases* because the free-volume per particle is larger in the ordered than in the disordered phase.

The most famous, and for a long time controversial, example of an entropy-driven ordering transition is the freezing transition in a system of hard spheres. This transition had been predicted by Kirkwood in the early fifties [20] on the basis of an approximate theoretical description of the hard-sphere model. As this prediction was quite counter-intuitive and not based on any rigorous theoretical results, it met with wide-spread skepticism until Alder and Wainwright [21] and Wood and Jacobson [22] performed numerical simulations of the hard-sphere system that showed direct evidence for this freezing transition. Even then, the acceptance of the idea that freezing could be an *entropy* driven transition, came only slowly [23]. However, by now, the idea that hard spheres undergo a first-order freezing transition is generally accepted.

Since the work of Hoover and Ree [25], we have known the location of the thermodynamic freezing transition. We now also know that the face-centered cubic phase is more stable than the hexagonal close-packed phase [26], but by only $10^{-3}k_BT$ per particle. To understand how little this is, consider the following: if we used calorimetric techniques to determine the relative stability of the *fcc* and *hcp* phases, we would find that the free-energy difference amounts to some 10^{-11} cal/cm^3! Moreover, computer simulations allow us to estimate the equilibrium concentration of point defects (in particular, vacancies) in hard-sphere crystals [27]. At melting, this concentration is small, but not very small (of the order of one vacancy per four-thousand particles).

The next surprise in the history of ordering due to entropy came in the mid-eighties when computer simulations [28] showed that hard-core interactions alone could also explain the formation of more complex liquid crystals. In particular, it was found that a system of hard sphero-cylinders (*i.e.* cylinders with hemi-spherical caps, see Figure 4) can form a smectic liquid crystal, in addition to the isotropic liquid, the nematic phase and the crystalline solid [29]. In the smectic (A) phase, the molecules are orientationally ordered but, in addition, the translational symmetry is broken: the system exhibits a

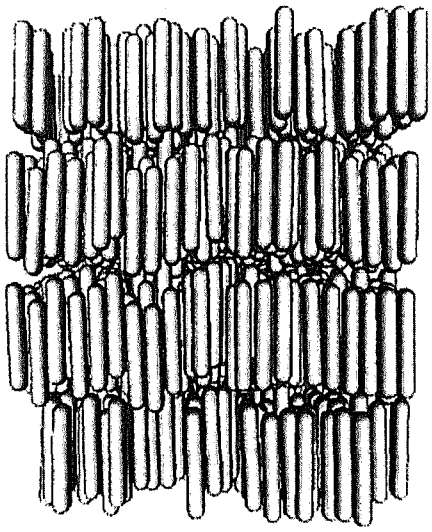

Figure 4. *Snapshot of a hard-core smectic liquid crystal.*

one-dimensional density-modulation. (See also Roux, this volume.) Subsequently, it was found that some hard-core models could also exhibit columnar ordering [30]. In the latter case, the molecules assemble in liquid-like stacks, but these stacks order to form a two-dimensional crystal. In summary, hard-core interaction can induce orientational ordering and one-, two- and three-dimensional positional ordering.

3.3 To boil—or not to boil...

Why do liquids exist? We are so used to the occurrence of phenomena such as boiling and freezing that we rarely pause to ask ourselves if things could have been different. Yet the fact that liquids must exist is not obvious *a priori.* This point is eloquently made in an essay by Weisskopf [31]:

> *The existence and general properties of solids and gases are relatively easy to understand once it is realised that atoms or molecules have certain typical properties and interactions that follow from quantum mechanics. Liquids are harder to understand. Assume that a group of intelligent theoretical physicists had lived in closed buildings from birth such that they never had occasion to see any natural structures. Let us forget that it may be impossible to prevent them to see their own bodies and their inputs and outputs. What would they be able to predict from a fundamental knowledge of quantum mechanics? They probably would predict the existence of atoms, of molecules, of solid crystals, both metals and insulators, of gases, but most likely not the existence of liquids.*

Weisskopf's statement may seem a bit bold. Surely, the liquid-vapour transition could have been predicted *a priori.* This is a hypothetical question that can never be answered. But, as I shall discuss below, in colloidal systems there may exist an analogous phase

transition that has not yet been observed experimentally and that was found in simulation before it had been predicted. To set the stage, let us first consider the question of the liquid-vapour transition. In his 1873 thesis, van der Waals gave the correct explanation for a well known, yet puzzling feature of liquids and gases, namely that there is no essential distinction between the two: above a critical temperature T_c, a vapour can be compressed continuously all the way to the freezing point. Yet below T_c, a first-order phase transition separates the dilute fluid (vapour) from the dense fluid (liquid) [32]. It is due to a the competition between short-ranged repulsion and longer-ranged attraction. From the work of Longuet-Higgins and Widom [35], we now know that the van der Waals model (in which molecules are described as hard spheres with an infinitely weak, infinitely long-ranged attraction [34]) is even richer than originally expected: it exhibits not only the liquid-vapour transition but also crystallisation (Figure 5).

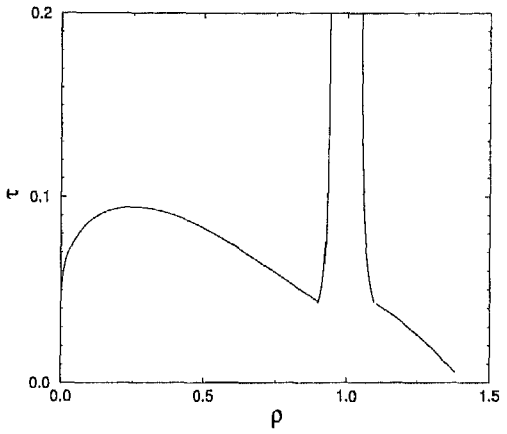

Figure 5. *Phase diagram of a system of hard spheres with a weak, long-range attraction (the 'true' van der Waals model). The density is expressed in units σ^{-3}, where σ is the hard-core diameter. The 'temperature' τ is expressed in terms of the van der Waals a-term: $\tau = k_B T v_0/a$, where v_0 is the volume of the hard spheres. (Hence the van der Waals mean-field equation of state reads $(p + aN/V)(V - Nv_0) = Nk_BT$). Plotted is the coexistence line: below this, vapour-liquid or fluid-crystal coexistence occurs.*

The liquid-vapour transition is possible between the critical point and the triple point, and in the van der Waals model, the temperature of the critical point is about a factor two large than that of the triple point. There is, however, no fundamental reason why this transition should occur in every atomic or molecular substance, nor is there any rule that forbids the existence of more than one fluid-fluid transition. Whether a given compound will have a liquid phase, depends sensitively on the range of the intermolecular potential: as this range is decreased, the critical temperature approaches the triple-point temperature, and when T_c drops below the latter, only a single stable fluid phase remains. In mixtures of spherical colloidal particles and non-adsorbing polymer, the range of the attractive part of the effective colloid-colloid interaction can be varied by changing the size of the polymers (see Section 2.6). Experiment, theory and simulation all suggest that when the width of the attractive well becomes less than approximately one third of the diameter of the colloidal spheres, the colloidal 'liquid' phase disappears.

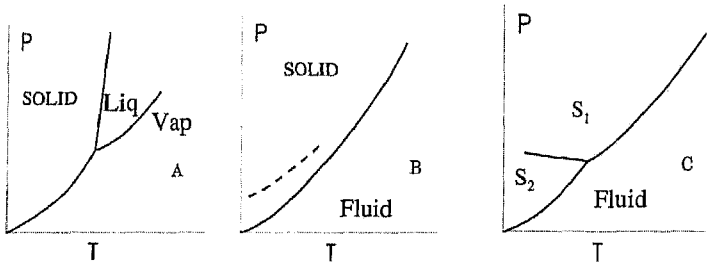

Figure 6. *Sequence of phase diagram for a system of spherical particles as the interaction range is varied. The range of the interaction decreases from left to right in the sequence. Diagram A is normal for a simple molecular substance (the liquid-vapour line ends in a critical point while the liquid-solid line continues indefinitely). In diagram B, the liquid-vapour line is metastable only, but can have dynamical consequences (see Section 5) (dotted). In diagram C, there is an isostructural solid-solid coexistence line.*

Figure 6 shows schematically the evolution of the phase-diagram of a system of spherical particles with a variable ranged attraction. As the range of attraction decreases, the liquid-vapour curve moves into the metastable regime. For very short-ranged attraction (less than 5% of the hard-core diameter), a first-order iso-structural solid-solid transition appears in the solid phase [36]. It should be stressed that phase diagrams of type **B** in figure 6 are common for colloidal systems, but rare for simple molecular systems. A possible exception is C_{60} [37]. Phase diagrams of type **C** have, thus far, not been observed in colloidal systems. Nor had they been predicted before the simulations appeared (this suggests that Weisskopf was right).

4 Colloid dynamics

For the computer simulator, the study of colloid dynamics is a challenge. The reason is that colloid dynamics spans a wide range of time-scales. No single simulation can cover all time-scales simultaneously. Below, I shall discuss two aspects of colloid dynamics that clearly illustrate the time-scale problem. The first is colloidal *hydrodynamics*. The second is homogeneous nucleation of a new phase from a metastable phase.

4.1 Hydrodynamic effects in colloidal suspensions

Colloid dynamics is a research field in its own right (see *e.g.* [38]). Clearly, I cannot cover this field in a few pages. I therefore wish to focus on a few simple concepts that are useful when thinking about the dynamics of colloidal particles. The analogy between colloids and atoms that is useful when discussing the static properties of colloidal matter, breaks down completely when discussing the dynamics. The reason is that atoms in a dilute gas phase move *ballistically*, colloids in a dilute suspension move *diffusively*. In order to understand the motion of colloids, we have to consider the hydrodynamic properties of the surrounding solvent. Just imagine what would happen if kinetic gas theory applied

to the motion of colloids: then the frictional force acting on a spherical colloid would be caused by independent collisions with the solvent molecules, and we would find that the frictional force is proportional to the velocity of the colloid, $\mathbf{v}$ (which is correct) and the effective area of the colloid (πa^2) (which is wrong). In fact, the true frictional force on a colloid moving at a constant velocity $\mathbf{v}$ is given by the Stokes expression

$$\mathbf{F}_{\text{frict}} = -6\pi\eta a\mathbf{v} \,, \tag{28}$$

where η is the viscosity of the solvent and a the radius of the colloid.

The Stokes relation can be derived from hydrodynamics, however this derivation does not make it intuitively obvious why the friction is proportional to a rather than to a^2. Below, I shall give a hand-waving derivation that is more intuitively appealing (although the answer is not quite right). We start with the assumption that the time evolution of any flow field $\mathbf{u}(\mathbf{r},t)$ in the solvent obeys the Navier-Stokes equation for an incompressible fluid

$$d_s\left(\frac{\partial \mathbf{u}(\mathbf{r},t)}{\partial t} + \mathbf{u}(\mathbf{r},t)\cdot\nabla\mathbf{u}(\mathbf{r},t)\right) = \eta\nabla^2\mathbf{u}(\mathbf{r},t) - \nabla p(\mathbf{r},t) \,,$$

where $\mathbf{u}(\mathbf{r},t)$ is the flow velocity at point $\mathbf{r}$ and time t, d_s is the mass density of the solvent and $p(\mathbf{r},t)$ is the hydrostatic pressure. I shall consider the case that $\mathbf{u}(\mathbf{r},t)$ is 'small' (low Reynolds-number regime, see [38]). Then we can neglect the $\mathbf{u}\cdot\nabla\mathbf{u}$ term. Let us now consider the situation where the solvent is in contact with a flat surface (see Figure 7). Initially, both fluid and wall are at rest. At time $t = 0$, the wall is given a tangential

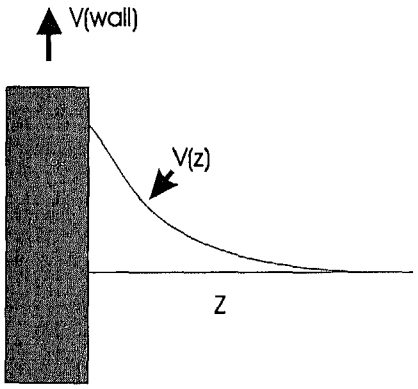

Figure 7. *When a wall is suddenly given a tangential velocity* $\mathbf{v}_{\text{wall}}$*, the transverse velocity field penetrates* diffusively *into the bulk fluid.*

velocity $\mathbf{v}_{\text{wall}}$. We assume that this velocity is parallel to the y-direction. The normal to the surface defines the z-direction. In this geometry, the equation of motion for the flow field reduces to

$$d_s\frac{\partial u_y(z,t)}{\partial t} = \eta\nabla_z^2 u_y(z,t) \,.$$

But this is effectively a *diffusion* equation for the transverse velocity. The 'diffusion coefficient' is equal to $(\eta/d_s) \equiv \nu$. This diffusion coefficient for transverse momentum is called

the *kinematic viscosity*. The larger ν is, the faster transverse momentum diffuses away from its source. Diffusion equations typically show up when we consider the transport of a quantity that is conserved, such as mass, energy or (in this case) momentum.

Let us now use this concept of diffusing momentum to estimate the frictional drag on a sphere. To simplify matters, I shall pretend that the transverse momentum is a *scalar* rather than a *vector*. Clearly, this is wrong, but it will not affect the qualitative answer. A moving sphere acts as a source of transverse momentum. The transverse momentum flux j_T is related to the gradient in the transverse velocity field (v_T) by

$$j_T = -\eta \nabla v_T \,.$$

In steady state, $\nabla^2 v_T(r) = 0$. If the transverse velocity were a scalar, the solution to this equation would be

$$v_T(r) = v_0 \frac{a}{r} \,, \tag{29}$$

where v_0 is the velocity of the colloidal sphere. The transverse momentum current density is then

$$j_T = \eta v_0 \frac{a}{r^2} \,.$$

The frictional force on the sphere is equal to minus the total rate at which momentum flows into the fluid

$$F_{\text{frict}} = -4\pi r^2 j_T = -4\pi\eta a v_0 \,, \tag{30}$$

which is almost Stokes' law (the factor 4π instead of 6π is due to our cavalier treatment of the vectorial character of the velocity).

This trivial example shows that the conservation of momentum is absolutely crucial for the understanding of colloid dynamics. A second result that follows almost immediately from Equation 29 is that the flow velocity at a distance r from a moving colloid, decays as $1/r$. Through this velocity field, one colloid can exert a drag force on another colloid. This is the so-called *hydrodynamic interaction*, and is very long ranged. Again, for a correct derivation, I refer the reader to [38].

Having established a simple language for the discussion of colloid dynamics, we can make estimates of the relevant time-scales that govern the time evolution of a colloidal system. The shortest time-scale τ_s, is usually not even considered. It is the time-scale on which the solvent behaves as a *compressible* fluid. If we set a colloid in motion, this will set up a density disturbance. This density modulation will be propagated away as a sound wave (carrying with it one third of the momentum of the colloid [38]). This sound wave will have moved away after a time $\tau_s = a/c_s$ (where c_s is the velocity of sound). Typically, $\tau_s = \mathcal{O}(10^{-10}\text{s})$. The next time-scale is the one associated with the propagation of hydrodynamic interactions: τ_H. It is of the order of the time it takes transverse momentum to diffuse a typical interparticle distance: $\tau_H = \mathcal{O}(\rho^{-2/3}/\nu)$, where ρ is the number density of the colloids. In dense suspensions, the typical inter-particle distance is comparable to the diameter of the colloids, and then $\tau_H = \mathcal{O}(a^2/\nu)$. Usually, this time-scale is of the order of 10^{-8}s. Next, we get the time-scale for the decay of the initial velocity of a colloid. If we assume (somewhat inconsistently, as it will turn out) that this decay

is determined by Stokes' law, we find that the decay of the velocity of a colloid occurs on a time-scale $\tau_v = \mathcal{O}(M_c/\eta a)$, where M_c is the mass of a colloid. Since $M_c = (4\pi a^3 d_c/3)$, where d_c is the mass density of the colloid, then we can write $\tau_v = \mathcal{O}(d_c a^2/\eta)$. In a dense suspension, $\tau_v = (d_c/d_s)\tau_H$. This means that, for a neutrally buoyant colloid, there is no separation in time-scales between τ_v and τ_H.

The final time-scale in colloid dynamics is the one associated with appreciable displacements of the colloids. As the colloids move diffusively, and as the diffusion constant is related to the Stokes friction constant by $D = k_B T/(6\pi\eta a)$, the time it takes a colloid to diffuse over a distance comparable to its own radius is $\tau_R = \mathcal{O}(a^2/D) \sim \mathcal{O}(\eta a^3)$. This τ_R is of the order of milliseconds to seconds. Clearly, there is a wide time-scale separation between τ_R and the other times. For times that are much longer than τ_v and τ_H, we can pretend that the colloids perform uncorrelated Brownian motion. However, this is not quite correct: even though the hydrodynamic interactions have long decayed, they render the effective diffusion constant of every colloid dependent on the instantaneous configuration of its neighbours. This is one of the reasons why the theory of colloid dynamics is not simple [38].

Let me, however, conclude this section on colloid dynamics with something that can easily be understood on the basis of diffusion of transverse momentum. The Stokes-Einstein relation provides an expression for the frictional force acting on a colloidal particle that moves at velocity v_c through the solvent: $F_{\text{fricf}} = -6\pi\eta a v_c$. At first sight, it appears that this equation allows us to compute the rate at which the initial velocity of a particle decays

$$M_c \frac{\partial v_c}{\partial t} = -6\pi\eta a v_c \,, \tag{31}$$

and the solution to this equation is

$$v_c(t) = v_c(0) \exp\left(-\frac{6\pi\eta a}{M_c} t\right) . \tag{32}$$

This answers looks reasonable. It even yields the correct expression for the diffusion constant. Indeed, using the Green-Kubo relation between the self-diffusion constant and the velocity-autocorrelation function $\langle v_x(0) v_x(t)\rangle$:

$$D = \int_0^\infty dt \langle v_x(0) v_x(t)\rangle \,, \tag{33}$$

we find $D = k_B T/(6\pi\eta a)$, as it should. Still, Equation 32 is wrong. Velocity fluctuations of colloidal particles (or, for that matter, even atoms [39]) do not decay exponentially, but with a power law.

In terms of the diffusive transport of transverse momentum, this is easy to understand. Consider a colloidal particle of mass M_c having an initial velocity v_c. Part of the initial momentum of the particle is carried away by sound waves (in fact, one third of the initial momentum). The remainder is converted to transverse momentum and is transported away diffusively. After a time t, the transverse momentum has diffused over a typical distance $\sqrt{2\nu t}$. That means that (two-thirds of) the initial momentum of the particle, $M_c v_c$ is now contained in a spherical volume with radius $\sqrt{2\nu t}$. This volume has a total

mass proportional to $d_s(\nu t)^{3/2}$. The average flow velocity of the fluid in this volume is equal to its momentum divided by its mass:

$$v_{av} \simeq \frac{M_c v_c}{d_s(\nu t)^{3/2}}. \tag{34}$$

The velocity of the colloidal particle is equal to this average flow velocity. Hence, for long times, the velocity-autocorrelation function of the colloidal particles decays as

$$\langle v_x(0)v_x(t)\rangle \simeq \frac{k_B T}{d_s(\nu t)^{3/2}}, \tag{35}$$

where we have used $\langle v_x^2(0)\rangle = k_B T/M_c$. As is clear from Equation 35, the velocity correlation function of a colloidal particle decays as $t^{-3/2}$. Several points should be noted: first of all, the decay described by Equation 35 can be, and has been, observed experimentally (see e.g. [40]). The power-law decay of the velocity auto-correlation function only describes the asymptotic behaviour. A similar analysis can be applied to the decay of the angular momentum of a rotating colloidal particle (in that case, the decay goes as $t^{-5/2}$ [41]). The presence of a wall perturbs the diffusion of transverse momentum. Using arguments very similar to the one above, one may then derive new power-law exponents for the decay of rotational and translational velocity correlation functions [42].

5 Metastability and nonequilibrium dynamics

It is well known that liquids can be supercooled before they freeze and vapours can be supersaturated before they condense: the resulting phases are *metastable*. Similar phenomena arise in colloids too. In what follows, we discuss the escape from such a metastable phase.

5.1 Homogeneous nucleation in colloidal suspensions

A homogeneous phase can be supercooled because the only route to the more stable state is via the formation of small *nuclei*. The free energy of such nuclei is determined not only by the difference in chemical potential between vapour and liquid, which drives the nucleation process, but also by their surface free energy. In classical nucleation theory (CNT) [43][44] it is assumed that the nuclei are compact, spherical objects, that behave like small droplets of bulk phase. The surface free energy term is always positive, because of the work that must be done to create an interface. Moreover, for small droplets this term dominates and hence the free energy of a nucleus increases with size. Only when the droplet has reached a certain critical size, does the volume term takes over, and the free energy decrease. It is only from here on that the nucleus grows spontaneously into a bulk liquid. The free energy of a spherical liquid droplet of radius R in a vapour is then given by

$$\Delta G = 4\pi R^2\gamma + \frac{4}{3}\pi R^3 \rho \Delta\mu, \tag{36}$$

where γ is the surface free energy, ρ is the particle number density in the bulk liquid, and $\Delta\mu$ is the difference in chemical potential between bulk liquid and bulk vapour. Clearly,

the first term on the right hand side of Equation 36 is the surface term, which is positive, and the second term is the volume term, which is negative; the difference in chemical potential is the driving force for the nucleation process. The height of the nucleation barrier can easily be obtained from the above expression, yielding

$$\Delta G^* = \frac{16\pi\gamma^3}{3\rho^2\Delta\mu^2}. \tag{37}$$

This equation shows that the barrier height depends not only on the surface free energy γ (and the density ρ), but also on the difference in chemical potential $\Delta\mu$. The difference in chemical potential is related to the supersaturation. Hence, the height of the free-energy barrier that separates the stable from the metastable phase depends on the degree of supersaturation. At coexistence, the difference in chemical potential is zero, and the height of the barrier is infinite. Although equally likely to be in the liquid or vapour phase, once the system is one state or the other, it will remain in this state; the system simply cannot transform into the other state.

Macroscopic thermodynamics dictates that the phase that is formed in a supersaturated system is the one that has the lowest free energy. However, nucleation is an essentially dynamic process, and therefore one cannot expect *a priori* that on supersaturating the system the thermodynamically most stable phase will be formed. In 1897, Ostwald [45] formulated his step rule, stating that the crystal phase that is nucleated from the melt need not be the one that is thermodynamically most stable, but the one that is closest in free energy to the fluid phase. Stranski and Totomanow [46] re-examined this rule and argued that the nucleated phase is the phase that has the lowest free-energy barrier of formation, under the conditions prevailing. The simulation results discussed below suggest that, even on a *microscopic* scale, something similar to Ostwald's step rule seems to hold.

5.2 Coil-globule transition in condensation of dipolar colloids?

The formation of a droplet of water from the vapour is probably the best known example of homogeneous nucleation of a polar fluid. However, the nucleation behaviour of polar fluids (including polar colloids) is still poorly understood. In fact, while classical nucleation theory gives a reasonable prediction of the nucleation rate of nonpolar substances, it seriously overestimates the rate of nucleation of highly polar compounds, such as acetonitrile, benzonitrile and nitrobenzene [47, 48]. In order to explain the discrepancy between theory and experiment, several nucleation theories have been proposed. It has been suggested that in the critical nuclei the dipoles are arranged in an anti-parallel head-to-tail configuration [47, 48], giving the clusters a non-spherical, prolate shape, which increases the surface-to-volume ratio and thereby the height of the nucleation barrier. In the oriented dipole model introduced by Abraham [49], it is assumed that the dipoles are perpendicular to the interface, yielding a size dependent surface tension due to the effect of curvature of the surface on the dipole-dipole interaction. However, in a density-functional study of a weakly polar Stockmayer fluid, it was found that on the liquid (core) side of the interface of critical nuclei, the dipoles are not oriented perpendicular to the surface, but parallel [50].

We have studied the structure and free energy of critical nuclei, as well as pre- and postcritical nuclei, of a highly polar Stockmayer fluid [51]. In the Stockmayer system,

the particles interact via a Lennard-Jones pair potential plus a dipole-dipole interaction potential

$$v(\mathbf{r}_{ij}, \boldsymbol{\mu}_i, \boldsymbol{\mu}_j) = 4\epsilon \left[\left(\frac{\sigma}{r_{ij}}\right)^{12} - \left(\frac{\sigma}{r_{ij}}\right)^{6} \right] - \frac{3(\boldsymbol{\mu}_i \cdot \mathbf{r}_{ij})(\boldsymbol{\mu}_j \cdot \mathbf{r}_{ij})}{r_{ij}^5} + \frac{\boldsymbol{\mu}_i \cdot \boldsymbol{\mu}_j}{r_{ij}^3}. \tag{38}$$

Here ϵ is the Lennard-Jones well depth, σ is the Lennard-Jones diameter, $\boldsymbol{\mu}_i$ denotes the dipole moment of particle i and $\mathbf{r}_{ij}$ is the vector joining particle i and j. We have studied the nucleation behaviour for reduced dipole moment $\mu^* = |\boldsymbol{\mu}|/\sqrt{\epsilon\sigma^3} = 4$, which is close to the value for water. We have computed [51] the excess free energy $\Delta\Omega$ of a cluster of size n in a volume V, at chemical potential μ and at temperature T, from the probability distribution function $P(n)$

$$\beta\Delta\Omega(n, \mu, V, T) \equiv -\ln[P(n)] = -\ln[N_n/N]. \tag{39}$$

Here β is the reciprocal temperature; N_n is the average number of clusters of size n and N is the average total number of particles. As the density of clusters in the vapour is low, the interactions between them can be neglected. As a consequence, we can obtain the free-energy barrier at any desired chemical potential μ' from the nucleation barrier measured at a given chemical potential μ via

$$\beta\Delta\Omega(n, \mu', V, T) = \beta\Delta\Omega(n, \mu, V, T) - \beta(\mu' - \mu)n + \ln\left[\rho(\mu')/\rho(\mu)\right], \tag{40}$$

where $\rho = N/V$ is the total number density in the system.

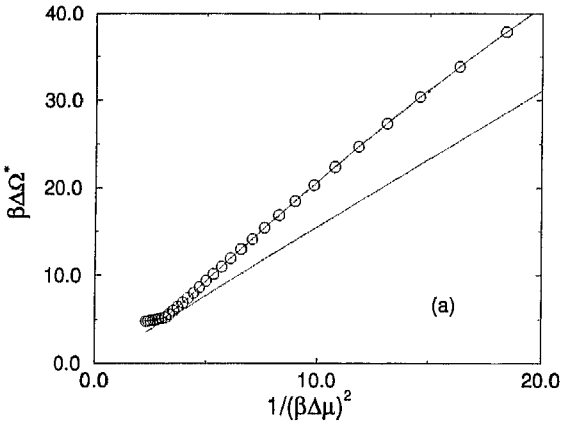

Figure 8. *Comparison of the barrier height between the simulation results (open circles) and classical nucleation theory (straight solid line) for a Stockmayer fluid with reduced dipole moment* $\mu^* = |\boldsymbol{\mu}|/\sqrt{\epsilon\sigma^3} = 4$ *and reduced temperature* $k_BT/\epsilon = 3.5$. *The chemical potential difference between the liquid and the vapour is* $\Delta\mu$.

Figure 8 shows the comparison between the simulation results and CNT for the height of the barrier. Clearly, the theory underestimates the barrier height. As the nucleation rate is dominated by the height of the barrier, our results are in qualitative agreement

with the experiments on strongly polar fluids [47, 48], in which it was found that CNT overestimates the nucleation rate. But, unlike the experiments, the simulations allow us to investigate the microscopic origins of the breakdown of classical nucleation theory.

In classical nucleation theory it is assumed that already the smallest clusters are compact, more or less spherical objects. In a previous simulation study on a typical nonpolar fluid, the Lennard-Jones fluid, we found that this is a reasonable assumption [52], even for nuclei as small as ten particles. However, the interaction potential of the Lennard-Jones system is isotropic, whereas the dipolar interaction potential is anisotropic. (On the other hand, the bulk liquid of this polar fluid is isotropic.) We find that the smallest clusters, that initiate the nucleation process, are not compact spherical objects, but chains, in which the dipoles align head-to-tail (Figure 9). In fact, we find a whole variety of differently

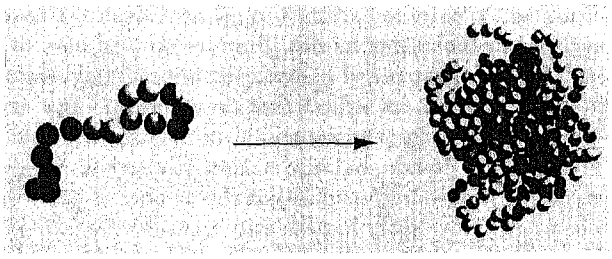

Figure 9. *Left: sub-critical nucleus in a supercooled vapour of dipolar spheres. The dipolar particles align head-to-tail. Right: critical nucleus. The chain has collapsed to form a more-or-less compact, globular cluster.*

shaped sub-critical clusters in dynamical equilibrium: linear chains, branched-chains, and 'ring-polymers'. Initially, as the cluster size is increased, the chains become longer. But, beyond a certain size, the clusters collapse to form a compact globule. The Stockmayer fluid is a simple model system for polar fluids and the mechanism that we describe here might not be applicable for all fluids that have a strong dipole moment. However, it is probably not a bad model for colloids with an embedded electrical or magnetic dipole. The simulations show that the presence of a sufficiently strong permanent dipole may drastically change the pathway for condensation.

5.3 Crystallisation near a metastable critical point

Proteins are notoriously difficult to crystallise. The experiments indicate that most proteins only crystallise under very specific conditions [54–56], otherwise remaining indefinitely as metastable, fluid suspensions. Moreover, the conditions are often not known beforehand. As a result, growing good protein crystals is a time-consuming business. Interestingly, there seems to exist a similarity between the phase diagram of globular proteins and of colloids with short-range attractive interactions [57]. In fact, a series of studies [58–61] show that the phase diagram of a wide variety of proteins is of the kind shown in Figure 6B. Rosenbaum and Zukoski [57, 62] observed that the conditions under which a large number of globular proteins can be made to crystallise, map onto a narrow temperature range of the computed fluid-solid coexistence curve of colloids with

short-ranged attraction [63]. If the temperature is too high, crystallisation is hardly observed at all, whereas if the temperature is too low, amorphous precipitation rather than crystallisation occurs. Only in a narrow window around the metastable liquid-vapour critical point, can high-quality crystals be formed. In order to grow high-quality protein crystals, the quench should be relatively shallow, and the system should not be close to a glass transition. Under these conditions, the rate-limiting step in crystal nucleation is the crossing of the free-energy barrier. Using simulation, it is possible to study the nucleation barrier, and the structure of the critical nucleus in the vicinity of this metastable critical point [64].

We performed simulations on a model system for particles with a short-ranged attraction, for a number of state points near the metastable critical point. These state-points were chosen such that on the basis of classical nucleation theory the same height of the barrier could be expected. In order to find the free-energy barrier, we have computed the free energy of a nucleus as a function of its size. However, we first have to define what we mean by a 'nucleus'. As we are interested in crystallisation, it might seem natural to use a crystallinity criterion. However, we expect that crystallisation near the critical point is influenced by critical density fluctuations within the metastable fluid. We therefore used not only a crystallinity criterion, but also a density criterion. We define the size of a high-density cluster (be it solid- or liquidlike) as the number of particles, N_ρ, within a connected region of significantly higher local density than the particles in the remainder of the system. The number of these particles that is also in a crystalline environment is denoted by $N_{\rm crys}$. In our simulations, we have computed the free-energy 'landscape' of a nucleus as a function of the two coordinates N_ρ and $N_{\rm crys}$.

Figure 10 shows the free-energy landscape for $T = 0.89T_c$ and $T = T_c$. We find that away from T_c (both above and below), the path of lowest free energy is one where the increase in N_ρ is proportional to the increase in N_{crys} (Figure 10A). Such behaviour is expected if the incipient nucleus is simply a small crystallite. However, around T_c, critical density fluctuations lead to a striking change in the free-energy landscape (Figure 10B). First, the route to the critical nucleus leads through a region where N_ρ increases while N_{crys} is still essentially zero. In other words: the first step towards the critical nucleus is the formation of a liquidlike droplet. Then, beyond a certain critical size, the increase in N_ρ is proportional to N_{crys}, that is, a crystalline nucleus forms inside the liquidlike droplet.

Clearly, the presence of large density fluctuations close to a fluid-fluid critical point has a pronounced effect on the route to crystal nucleation. But, more importantly, the nucleation barrier close to T_c is much lower than at either higher or lower temperatures (Figure 11). The observed reduction in ΔG^* near T_c by some $30k_BT$ corresponds to an increase in nucleation rate by a factor 10^{13}. Finally, let us consider the implications of this reduction of the crystal nucleation barrier near T_c. An alternative way to lower the crystal nucleation barrier would be to quench the solution deeper into the metastable region below the solid-liquid coexistence curve. However, such deep quenches often result in the formation of amorphous aggregates [57, 61, 62, 65–68]. Moreover, in a deep quench, the thermodynamic driving force for crystallisation ($\mu_{\rm liq} - \mu_{\rm cryst}$) is also enhanced. As a consequence, the crystallites that nucleate will grow rapidly and far from perfectly [55]. Thus the nice feature of crystal nucleation in the vicinity of the metastable critical point is, that crystals can be formed at a relatively small degree of undercooling. It should be

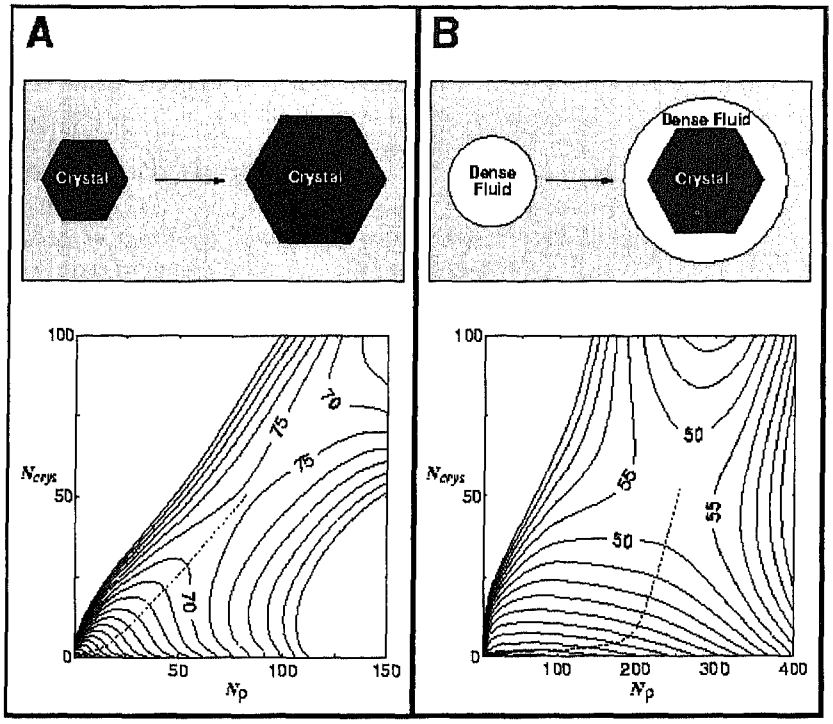

Figure 10. *Contour plots of the free-energy landscape along the path from the metastable fluid to the critical crystal nucleus, for our system of spherical particles with short-ranged attraction. The curves of constant free energy are drawn as a function of N_ρ and N_{crys} (see text) and are separated by $5k_BT$. If a liquidlike droplet forms in the system, we expect N_ρ to become large, while N_{crys} remains essentially zero. In contrast, for a normal crystallite, we expect that N_ρ is proportional to N_{crys}. Panel A shows the free energy landscape well below the critical temperature ($T/T_c = 0.89$). The lowest free-energy path to the critical nucleus is indicated by a dashed curve. Note that this curve corresponds to the formation and growth of a highly crystalline cluster. Panel B: The same, but now for $T = T_c$. In this case, the free-energy valley (dashed curve) first runs parallel to the N_ρ axis (formation of a liquid-like droplet), and moves towards a structure with a higher crystallinity (crystallite embedded in a liquid-like droplet). The free energy barrier for this route is much lower than the one shown in A.*

stressed that nucleation will also be enhanced in the vicinity of the fluid-fluid *spinodal*. Hence, there is more freedom in choosing the optimal crystallisation conditions. Finally, I note that in colloidal (as opposed to protein) systems, the system tends to form a gel before the metastable fluid-fluid branch is reached. A possible explanation for the difference in behaviour of proteins and colloids is discussed in [69].

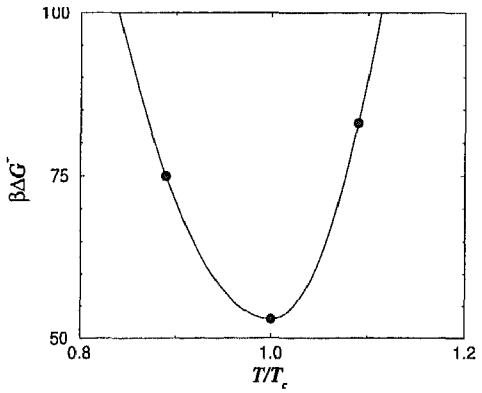

Figure 11. *Variation of the free-energy barrier for homogeneous crystal nucleation, as a function of T/T_c, in the vicinity of the critical temperature. The solid curve is a guide to the eye. The simulations show that the nucleation barrier goes through a minimum around the metastable critical point (see text).*

5.3.1 Microscopic step rule

Ostwald formulated his step rule more than a century ago [45] on the basis of macroscopic studies of phase transitions. The simulations suggest that also on a microscopic level, a 'step rule' may apply and that metastable phases may play an important role in nucleation. We find that the structure of the pre-critical nuclei is that of a metastable phase (chains/liquid). As the nuclei grow, the structure in the core transforms into that of the stable phase (liquid/fcc-crystal). Interestingly, in the interface of the larger nuclei traces of the structure of the smaller nuclei are retained.

5.4 Concluding remarks on nucleation dynamics

The reader may have noticed that I have discussed the subject of homogeneous nucleation without ever discussing the actual *dynamics* of the barrier-crossing process. The reason is that usually (well away from the gelation point) the barrier height completely dominates the variation of the nucleation rate. However, in a full description of nucleation in colloids, the actual dynamics of the barrier crossing process should be taken into account. (See McLeish, this volume, for similar remarks in a different, polymeric context.) Computationally, this is feasible, but non-trivial—after all, the dynamics of colloids in suspension is itself quite complex. But the techniques to study this problem exist.

6 Conclusion

Finally: I realise that my introduction to colloid physics has been biased and superficial. Biased because, as a simulator, I tend to focus on idealised models. Superficial because, wherever I could, I gave quick-and-dirty explanations instead of decent derivations. As much as possible, I have tried to refer the reader to the 'correct' literature. But, as these

lectures are not meant to be an exhaustive review, I have surely omitted many more relevant references than I have quoted. I hope that both the reader and the offended authors will forgive me.

Acknowledgments

The work of the FOM Institute is part of the research program of Stichting Fundamenteel Onderzoek der Materie (FOM) and is supported by NWO. I gratefully acknowledge the contributions of numerous students postdocs and colleagues, in particular: Alain Stroobants, Alfons van Blaaderen, Ard Louis, Bela Mulder, Chris Lowe, David Kofke, David Oxtoby, Emmanuel Trizac, Evert Jan Meijer, Henk Lekkerkerker, Ignacio Pagonabarraga, James Polson, Jan Veerman, Jeroen van Duijneveldt, Jose Cuesta, Maarten Hagen, Maria-Jose Ruiz-Montero, Marjolein Dijkstra, Martin van der Hoef, Martin Bates, Massimo Noro, Mike Allen, Norbert Kern, Peter Bladon, Peter Bolhuis, Pieter Rein ten Wolde, Richard Sear, Sander Pronk, Thierry Biben and Tony Ladd.

References

[1] L Onsager, *Ann NY Acad Sci* **51** 627 (1949)

[2] E J Verwey and J Th G Overbeek, *Theory of the Stability of Lyophobic Colloids* (Elsevier, Amsterdam, 1948)

[3] I Sogami and N Ise, *J Chem Phys* **81** 6320 (1984)

[4] A E Larsen and D G Grier, *Nature* **385** 230–233 (1997)

[5] G M Kepler and S Fraden, *Phys Rev Lett* **73** 356 (1994)

[6] W R Bowen and A O Sharif, *Nature* **393** 663–665 (1998)

[7] D Goulding and J P Hansen, *Europhys Lett* **46** 407 (1999)

[8] J C Neu, *Phys Rev Lett* **82** 1072 (1999)

[9] R vanRoij and J P Hansen, *Phys Rev Lett* **79** 3082 (1997),
R van Roij, M Dijkstra and J P Hansen, *Phys Rev E* **59** 2010 (1999)

[10] J Ray and G S Manning, *Langmuir* **10** 2450 (1994),
J L Barrat and J F Joanny, *Adv Chem Phys* **94** 1 (1996),
N Grønbech-Jensen, R J Mashl, R F Bruinsma, and W M Gelbart, *Phys Rev Lett* **78** 2477 (1997),
B-Y Ha and Andrea J Liu, *Phys Rev Lett* **79** 1289 (1997) and *Phys Rev Lett* **81** 1011 (1998)

[11] J Israelachvili, *Intermolecular and Surface Forces*, 2nd edn (Academic Press, London, 1992)

[12] D Frenkel and A A Louis, *Phys Rev Lett* **68** 3363 (1992). In fact, in a different context, this model had been introduced by B Widom, *J Chem Phys* **46** 3324 (1967)

[13] L Onsager, *Phys Rev* **65** 117 (1944)

[14] S Asakura and F Oosawa, *J Chem Phys* **22** 1255 (1954); *J Polym Sci* **33** 183 (1958)

[15] A Vrij, *Pure Appl Chem* **48** 471 (1976)

[16] A P Gast, C K Hall and W B Russel, *J Colloid Interface Sci* **96** 251 (1983)

[17] H N W Lekkerkerker, W C Poon, P N Pusey, A Stroobants and P B Warren, *Europhysics Lett* **20** 559 (1992)

[18] E J Meijer and D Frenkel, *Phys Rev Lett* **67** 1110 (1991), *J Chem Phys* **100** 6873–6887 (1994), *Physica A* **213** 130–137 (1995)

[19] M A Bates and D Frenkel, *J Chem Phys* **109** 6193 (1998)

[20] J E Kirkwood in *Phase Transformations in Solids*, R Smoluchowski, J E Mayer and W A Weyl (eds),Wiley, New York (1951), p 67

[21] B J Alder and T E Wainwright, *J Chem Phys* **27** 1208 (1957)

[22] W W Wood and J D Jacobson, *J Chem Phys* **27** 1207 (1957)

[23] *The Many-Body Problem*, J K Percus, editor, Interscience, New York, 1963

[24] P N Pusey, in *Liquids, freezing and glass transition*, J P Hansen, D Levesque and J Zinn-Justin (editors),North-Holland, Amsterdam, 1991, p 763

[25] W G Hoover and F H Ree, *J Chem Phys* **49** 3609–3617 (1968)

[26] P G Bolhuis, D Frenkel, S-C Mau and D A Huse, *Nature* **388** 235 (1997)

[27] C H Bennett and B J Alder, *J Chem Phys* **54** 4796 (1970)

[28] D Frenkel, H N W Lekkerkerker and A Stroobants, *Nature* **332** 822 (1988)

[29] Peter Bolhuis and Daan Frenkel, *J Chem Phys* **106** 666 (1997)

[30] J A C Veerman and D Frenkel, *Phys Rev* **A45** 5633 (1992)

[31] V F Weissskopf, *Trans NY Acad Sci II*, **38**, 202 (1977)

[32] J S Rowlinson, *Studies in Statistical Mechanics* Vol XIV, J L Lebowitz (editor), North Holland, Amsterdam, 1988

[33] R F Kayser and H J Raveche, *Phys Rev* **A17** 2067 (1978)

[34] P C Hemmer and J L Lebowitz, in *Critical Phenomena and Phase Transitions* **5b**, C Domb and M Green (editors), Academic Press, New York, (1976)

[35] H C Longuet-Higgins and B Widom, *Mol Phys* **8** 549 (1964)

[36] P G Bolhuis and D Frenkel, *Phys Rev Lett* **72**, 221 (1994)
P G Bolhuis, M H J Hagen and D Frenkel, *Phys Rev* **E50** 4880 (1994)

[37] M H J Hagen, E J Meijer, G C A M Mooij, D Frenkel and H N W Lekkerkerker, *Nature*, **365** 425 (1993)

[38] J K G Dhont, *An Introduction to Dynamics of Colloids*, Elsevier, Amsterdam, 1996

[39] B J Alder and T E Wainwright, *Phys Rev A* **1** 18 (1970)

[40] J X Zhu, D J Durian, J Muller, D A Weitz and D J Pine, *Phys Rev Lett* **68** (16) 2559 (1992)

[41] C P Lowe, D Frenkel and A J Masters, *J Chem Phys* **103** 1582 (1995)

[42] I Pagonabarraga, M H J Hagen, C P Lowe and D Frenkel, *Phys Rev E* **58** 7288 (1998)

[43] M Volmer and A Weber, *Z Phys Chem* **119** 227 (1926)

[44] R Becker and W Döring, *Ann Phys* **24** 719 (1935)

[45] W Ostwald, *Z Phys Chem* **22** 289 (1897)

[46] I N Stranski and D Totomanow, *Z Physikal Chem* **163** 399 (1933)

[47] D Wright, R Caldwell, C Moxeley, and M S El-Shall, *J Chem Phys* **98** 3356 (1993)

[48] D Wright and M S El-Shall, *J Chem Phys* **98** 3369 (1993)

[49] F F Abraham, *Science* **168** 833 (1970)

[50] V Talanquer and D W Oxtoby, *J Chem Phys* **99** 4670 (1993)

[51] P R ten Wolde, D W Oxtoby and D Frenkel, *Phys Rev Lett* **81** 3695 (1998)

[52] P R ten Wolde and D Frenkel, *J Chem Phys* **109** 9901 (1998)

[53] I Kusaka, Z-G Wang, and J H Seinfeld, *J Chem Phys* **108** 3446 (1998)

[54] A McPherson, *Preparation and Analysis of Protein Crystals*, Krieger Publishing, Malabar (1982)

[55] S D Durbin and G Feher, *Ann Rev Phys Chem* **47** 171 (1996)

[56] F Rosenberger, *J Crystal Growth* **166** 40 (1996)

[57] D Rosenbaum, P C Zamora, and C F Zukoski, *Phys Rev Lett* **76** 150 (1996)

[58] C R Berland, G M Thurston, M Kondo, M L Broide, J Pande, O O Ogun, and G B Benedek, *Proc Natl Acad Sci USA* **89** 1214 (1992)

[59] N Asherie, A Lomakin, and G B Benedek, *Phys Rev Lett* **77** 4832 (1996)

[60] M L Broide, T M Tominc, and M D Saxowsky, *Phys Rev E* **53** 6325 (1996)

[61] M Muschol and F Rosenberger, *J Chem Phys* **107** 1953 (1997)

[62] D Rosenbaum and C F Zukoski, *J Crystal Growth* **169** 752 (1996)

[63] M H J Hagen and D Frenkel, *J Chem Phys* **101** 4093 (1994)

[64] P R ten Wolde and D Frenkel, *Science* **277** 1975 (1997)

[65] A George and W W Wilson, *Acta Crytallogr* **D50** 361 (1994)

[66] S M Ilett, A Orrock, W C K Poon and P N Pusey, *Phys Rev E* **51** 1344 (1995)

[67] W C K Poon, A D Pirie, and P N Pusey, *Faraday Discuss* **101** 65 (1995)

[68] W C K Poon, *Phys Rev* **E55** 3762 (1997)

[69] M Noro, N Kern and D Frenkel, *Europhysics Lett* (in press, 1999)